

Preparation and characterization of a biologic scaffold and hydrogel derived from colonic mucosa

Timothy J. Keane,^{1,2} Jenna Dziki,^{1,2} Arthur Castelton,¹ Denver M. Faulk,^{1,2} Victoria Messerschmidt,¹ Ricardo Londono,¹ Janet E. Reing,¹ Sachin S. Velankar,³ Stephen F. Badylak^{1,2,4}

¹McGowan Institute for Regenerative Medicine, Pittsburgh, Pennsylvania 15219

²Department of Bioengineering, University of Pittsburgh, Pittsburgh, Pennsylvania 15213

³Department of Chemical and Petroleum Engineering, University of Pittsburgh, Pittsburgh, Pennsylvania 15213

⁴Department of Surgery, University of Pittsburgh, Pittsburgh, Pennsylvania 15219

Received 30 June 2015; revised 28 August 2015; accepted 11 October 2015

Published online 27 October 2015 in Wiley Online Library (wileyonlinelibrary.com). DOI: 10.1002/jbm.b.33556

Abstract: Gastrointestinal pathologies, injuries, and defects affect millions of individuals each year. While there are diverse treatment options for these individuals, no ideal solution exists. The repair or replacement of gastrointestinal tissue, therefore, represents a large unmet clinical need. Biomaterials derived from extracellular matrix (ECM) scaffolds have been effectively used to repair or replace numerous tissues throughout the body in both preclinical and clinical studies. Such scaffolds are prepared from decellularized tissues, and the biochemical, structural, and biologic properties vary depending upon the source tissue from which the ECM is derived. Given the potential benefit of a site-specific ECM scaffold for some applications, the objective of

this study was to prepare, characterize, and determine the *in vitro* and *in vivo* cell response to ECM derived from porcine colon. Results of this study show that porcine colon can be effectively decellularized while retaining biochemical and structural constituents of the source tissue. Two forms of colonic ECM, scaffold and hydrogel, were shown to be cell friendly and facilitate the polarization of macrophages toward an M2 phenotype both *in vitro* and *in vivo*. © 2015 Wiley Periodicals, Inc. *J Biomed Mater Res Part B: Appl Biomater*, 105B: 291–306, 2017.

Key Words: regenerative medicine, extracellular matrix, hydrogel, scaffolds

How to cite this article: Keane TJ, Dziki J, Castelton A, Faulk DM, Messerschmidt V, Londono R, Reing JE, Velankar SS, Badylak SF. 2017. Preparation and characterization of a biologic scaffold and hydrogel derived from colonic mucosa. *J Biomed Mater Res Part B* 2017;105B:291–306.

INTRODUCTION

The gastrointestinal (GI) tract is composed of a series of hollow muscular tubes that perform a variety of functions including mastication, digestion, motility, nutrient absorption, and waste excretion, among others. Such functional diversity requires organization of specialized cell and tissue types, and repair following injury or disease is imperative for the health of the host. Pathologies such as inflammatory bowel disease affect up to 4 million patients per year¹ and short bowel syndrome affects an additional 20,000 individuals in the United States alone.² Diseases such as these have very limited therapeutic options and are the cause of tremendous morbidity and health-care expenditures. Biomaterials and/or regenerative medicine strategies to address such problems will require the creation of a microenvironment that supports the cultivation, recruitment, differentiation, and maintenance of the specialized cell types required for normal GI function.

Biomaterial-mediated approaches to GI replacement must not only provide a mechanical support structure for cell growth but also be amenable to cell infiltration, allow for gas and nutrient exchange, and be compatible with the host innate immune system. Both synthetic and biologic scaffold materials have been manufactured and studied for GI repair/replacement applications and each are associated with their respective advantages and disadvantages.^{3,4} Synthetic scaffolds such as polylactic acid or polycaprolactone allow for tunable materials that can be tailored for specific applications. However, synthetic scaffolds invariably elicit proinflammatory and/or a foreign body response upon implantation that may result in encapsulation, fibrosis, and loss of function.⁵ Compatibility of scaffold materials with the host immune system has been shown to be a critical determinant of downstream functional tissue remodeling.⁶

Biologic scaffold materials, such as those composed of extracellular matrix (ECM) derived via decellularization of

Correspondence to: S. F. Badylak; e-mail: badylaks@upmc.edu

Contract grant sponsor: National Science Foundation (NSF) graduate research fellowship program; contract grant numbers: 1247842 (to T. J. K. and D. M. F.), BET 09320901 and 1336311 (to S. S. V.)

source tissues, can provide a compatible and instructive template for endogenous cell infiltration and differentiation, recapitulate the natural niche, and degrade to allow for complete host tissue replacement with associated release or exposure of bioactive matricryptic peptide sites. Implanted ECM bioscaffolds promote a favorable host immune response by induction of an M2-like macrophage phenotype. This immune modulation is typically associated with a functional constructive remodeling outcome. However, the properties and composition of ECM bioscaffolds are often variable and are critically dependent on factors such as source tissue anatomic site and age,⁷ use of chemical cross-linking agents,^{8,9} method of decellularization,¹⁰ manufacturing processes, and terminal sterilization methods.¹¹ The potential benefits of utilizing ECM scaffolds derived from homologous source tissue include the retention of tissue-specific cell phenotypes,^{12,13} enhancing tissue-specific differentiation,¹⁴ and promoting chemotaxis and proliferation of progenitor cells.¹⁵ Previous reports have shown that regions of the porcine GI system such as the small intestine [that is, small intestinal submucosa (SIS)] and esophagus can be decellularized and retain essential ultrastructural components, endogenous growth factors, and biomechanical strength.^{16–23} The suitability of these scaffolds for GI repair applications including treatment of esophageal disease, short bowel syndrome, ulcerative colitis, Crohn's disease, or mucositis, has not been extensively investigated. The various forms of these scaffold materials, including the intact sheet or tubular configuration, and the hydrogel configuration may prove useful for the traumatic and immune-mediated pathologies of the gut tract.

The objective of this study was to prepare, characterize, and determine the *in vitro* and *in vivo* cytocompatibility of ECM bioscaffolds derived from porcine colon. DNA content, retention of ultrastructural and biochemical molecules, biomechanical properties, *in vitro* cytocompatibility, and the *in vivo* host macrophage response were examined both quantitatively and qualitatively and compared across sheet, hydrogel, crosslinked, and incompletely decellularized forms of porcine colon ECM.

MATERIALS AND METHODS

Preparation of colonic ECM (coECM)

Colons were collected from market weight pigs (approximately 6 months of age and 260 lbs) at a local abattoir (Thoma's Meat Market, Saxonburg, PA). The colon was rinsed in water to remove contents and frozen at -20°C until use. Colonic submucosa was mechanically isolated from the surrounding tissue and then delipidized and decellularized. Native colonic submucosa prior to delipidization and decellularization was used as a control group. For the preparation of coECM, submucosa was depilidized with 2:1 (v/v) chloroform:methanol (30 min with stirring) followed by 3 washes each of 100%, 90%, and 70% ethanol (5 min per wash). The tissue was then rinsed in deionized water (3×5 min) and subjected to the following series of enzyme/detergent agitated baths: 0.02% Trypsin/0.05% EDTA (1 h at 37°C), 4% sodium deoxycholate (30 min), 4%

sodium deoxycholate (30 min), with water washes between each step (2×5 min). Finally, the decellularized tissue was disinfected in 0.1% peracetic acid/4% ethanol (2 h) and rinsed in phosphate-buffered saline (PBS; 2×15 min) and deionized water (2×15 min). Solutions were agitated on a shaker at 300 rpm and room temperature unless otherwise stated.

A subset of coECM scaffolds was subjected to chemical crosslinking (XL) using 10 mM N-(3-dimethylaminopropyl)-N'-ethylcarbodiimide hydrochloride (pH = 7) in PBS for 24 h at room temperature with constant stirring. The XL-coECM was then washed extensively in PBS for 48 h with stirring and then lyophilized to dry. For *in vitro* cell growth, *in vivo* implants, and suture retention strength experiments, the colonic submucosa, XL-coECM, and coECM were vacuum pressed to form a four-layer device. The devices used for cell culture and *in vivo* implantation were sterilized by ethylene oxide.

Hydrogel preparation

Hydrogels were prepared from coECM as previously described.²⁴ Briefly, lyophilized scaffolds were powdered using a Wiley Mill and filtered through a 60-mesh screen (<250 μm particle size). The comminuted ECM was then digested in 1 mg/mL porcine pepsin (Sigma Aldrich, St. Louis, MO) in 0.01*N* HCl for 48 h under constant stir rate at room temperature. Gelation was induced by neutralization of pH and salt concentration at 4°C . Specifically the addition of one-tenth digest volume of 0.1*N* NaOH and one-ninth digest volume of 10× PBS was used to bring pH to 7.4, phosphate buffer to 0.01*M*, and sodium chloride concentration to 0.15*M*. Gelation was then achieved by placing the neutralized digest in a nonhumidified incubator at 37°C for 1 h for *in vitro* studies. Gelation of coECM hydrogels for *in vivo* studies was accomplished by direct injection of the neutralized digest over the site of abdominal wall defect. ECM concentrations of 4 and 8 mg/mL were evaluated by turbidometric and rheologic assays. Cell culture and *in-vivo* experiments were conducted with 8 mg/mL coECM hydrogels.

Determining decellularization efficacy

Histologic analysis. Scaffolds (native colonic submucosa and coECM) and native colon tissue were fixed in 10% neutral buffered formalin for 24 h. The fixed samples were then paraffin embedded, and 5 μm sections were cut onto slides. Slides were stained with hematoxylin and eosin (H&E) or 4',6-diamidino-2-phenylindole (DAPI) to visualize the presence of nuclear material.

DNA concentration and fragment length analysis. Residual DNA content of the ECM was quantified by powdering samples with a Wiley Mill using a 60-mesh from separate preparations ($n = 4$) of lyophilized coECM. Samples (100 mg) were digested in 0.1 mg/mL proteinase K digestion buffer at 50°C for 24 h. DNA was extracted twice in phenol/chloroform/isoamyl alcohol and centrifuged at 10,000*g* (10 min at 4°C). The aqueous phase, containing the DNA,

was then mixed with 3M sodium acetate and 100% ethanol, frozen on dry ice for 20 min, centrifuged at 10,000*g* (10 min at 4°C), pouring off the supernatant, adding 70% ethanol, repeating centrifugation, removing supernatant, and drying the remaining DNA pellet. When dry, the pellet was resuspended in TE buffer (10 mM Tris/1 mM EDTA), and the DNA concentration was quantified utilizing a PicoGreen Assay (Invitrogen) following manufacturer's instructions. The fragment length of remnant DNA in the samples was then visualized with gel electrophoresis on a 1% agarose gel with a 100-bp ladder (Invitrogen) containing ethidium bromide.

Phospholipid measurement. Homogenates were prepared from 40 mg of lyophilized and comminuted tissue or ECM in 2 mL of homogenization buffer (50 mM Tris pH 7.4/20 mM CaCl₂/0.5% Triton X-100). Samples were homogenized on ice (15 s × 5) using a PowerGen 500 Homogenizer (Fisher Scientific, Pittsburgh, PA). Samples were centrifuged at 2000*g* for 20 min at 4°C, and the supernatant extract was collected. A second extraction was completed on the remaining pellet, as above, using 1 mL of extraction buffer. The extracts were combined and measured for phospholipid content using EnzyChrom Phospholipid Assay Kit (BioAssay Systems, Hayward, CA) according to manufacturer's instructions.

Glycosaminoglycan and growth factor measurement

The concentration of sulfated glycosaminoglycan (sGAG) and nonsulfated GAG in coECM samples was determined using the Blyscan Sulfated Glycosaminoglycan Assay Kit (Biocolor, Ltd., Belfast, Northern Ireland) and Hyaluronan Quantikine ELISA Kit (R&D Systems, Minneapolis, MN), respectively. The concentration of nonsulfated GAG, hyaluronic acid (HA), was measured using neutralized pepsin digests as described earlier. Digested samples were assayed following the manufacturer's protocol, and the assay was performed in duplicate on three different coECM samples.

The concentration of basic fibroblast growth factor (bFGF) and vascular endothelial growth factor (VEGF) in urea-heparin extracts of coECM samples was determined with the Quantikine Human FGF basic Immunoassay, Human VEGF Immunoassay (R&D Systems). Each assay for bFGF and VEGF was performed in quadruplicate. The ELISA assays are cross-reactive with porcine growth factors and do not measure activity.

Immunohistochemistry

Antigen retrieval was performed on deparaffinized slides with 5 µm sections using a 0.01M citrate buffer (pH = 6) heated to 95–100°C. Slides were placed in the hot buffer for 20 min and subsequently rinsed in PBS (3 × 5 min). Sections were placed in pepsin solution (0.05% pepsin/0.01M HCl) at 37°C for 15 min. After rinsing in PBS (3 × 5 min), the samples were blocked in blocking buffer (2% goat serum/1% bovine serum albumin/0.1% Triton X-100/0.1% Tween) for 1 h at room temperature. The sections were then incubated in the blocking buffer with rabbit polyclonal

laminin antibody (1:200 dilution; Abcam) or mouse monoclonal fibronectin (1:200 dilution; Abcam) overnight at 4°C in a humidified chamber. Sections were subsequently rinsed in PBS (3 × 5 min). Endogenous peroxidase activity was quenched by rinsing sections in a 3% hydrogen peroxide in methanol solution for 30 min followed by rinsing in PBS (3 × 5 min). Biotinylated goat anti-rabbit or goat anti-mouse secondary antibodies (Vector Laboratories, Burlingame, CA) were diluted 1:200 in blocking buffer and added to the sections for 30 min at 25°C and sections were subsequently rinsed in PBS (3 × 5 min). The slides were then incubated in detection solution (VectaStain® Elite ABC Reagent, Vector Laboratories) for 30 min at 37°C. After rinsing the slides, peroxidase substrate, 3,3'-diaminobenzidine (ImmPACT™ DAB; Vector Laboratories) was prepared per manufacturer instructions, and slides were incubated while being visualized under a microscope to time the color change for subsequent section staining. Tissues were rinsed in water (3 × 5 min). Sections were dipped in hematoxylin (Thermo Shandon, Pittsburgh, PA) for 1 min for a nuclear counterstain and subsequently rinsed in PBS (3 × 5 min).

Scanning electron microscopy

Scanning electron microscopy (SEM) was used to examine the surface topology of the luminal and abluminal sides of native porcine colonic tissue, submucosal tissue, and coECM. Samples were fixed in 2.5% glutaraldehyde in 1× PBS for 60 min, cut into blocks of 8 mm³, and washed thoroughly in 1× PBS three times at 15 min each. Samples were then fixed in 1% OsO₄ in PBS for 15 min each, dehydrated in graded series of alcohol (30–100%) baths for 15 min each. Samples were then critically point dried with hexamethyldisiloxane, mounted on studs, sputter coated, and stored in a desiccator until imaged. SEM images were captured using a JEOL 6335F Field Emission SEM instrument with a back-scatter detector.

Mechanical testing of coECM scaffolds

Planar biaxial testing. Planar biaxial mechanical testing was performed as previously described.²⁵ Briefly, a 15-mm × 15-mm sample of each tested material was acquired. Thickness was measured from the center of each material using a Starrett® caliper model 1010. Four fiducial markers were placed in the center of the square on the luminal surface after the removal of excess loose connective tissue and fat. Deformations were measured optically by tracking this four-marker array. Two loops of suture of equal length were attached to each side of the specimens with four stainless steel hooks, and 500 g Model 31 load cells (Honeywell) were used to acquire load values. Biaxial testing was conducted with the circumferential and longitudinal specimen axes aligned with the device axis and submerged in a bath at room temperature. The biaxial testing system was automated, allowing the marker locations and axial forces to be continuously recorded with custom marker tracking and data acquisition software.²⁶

Specimens were first preconditioned by cyclically loading the specimens to the desired maximum equibiaxial

stress of 250 kPa for 10 cycles using a cycle time of 30 s per cycle to quantify the quasi-static response. Immediately following the preconditioning cycles, the specimen was completely unloaded and imaged in its postpreconditioned free-floating configuration. The stress–stretch plot reported in this study start from a 5-g preload that is referenced to the postprecondition free float state, which was used to ensure test response repeatability. The response of the eight samples from each group was averaged after a three-point linear interpolation at representative stress values and reported with standard error. The maximum strain for each sample was then defined as the strain at the maximum tested stress of 250 kPa.

Suture retention testing. The suture retention test has been previously described.²⁷ The suture retention strength was performed according to ANSI/AAMI VP20-1994 Guidelines for Cardiovascular Implants-Vascular Prostheses. The suture retention strength was defined as the force required to pull a suture through the full thickness of the material. A 2-0 Prolene suture with a SH taper needle was passed through the test article with a 2-mm bite depth using a simple suture technique. The specimen was clamped at one end while the suture was attached to the uniaxial mechanical testing machine (Instron Model 3345 single column materials testing system) and pulled at a constant rate of 10 cm/min according to the aforementioned standard. Two tests were performed 1.5 cm apart on the same edge of the test article, and the maximum load was recorded for each test.

Rheologic testing of coECM hydrogels

The rheological characteristics of coECM hydrogels at 4 and 8 mg/mL were determined with a rheometer (AR2000, TA instruments, New Castle, DE) operating with 40-mm parallel plate geometry. The temperature was controlled within 0.1°C using a Peltier plate. Pregels were pH neutralized on ice and were immediately loaded onto the rheometer plate precooled to 10°C. Mineral oil was spread along the edge (i.e., the free surface of the hydrogel) to minimize evaporation. After loading, the steady shear viscosity was measured by applying a stress of 1 Pa at a frequency of 0.159 Hz. The temperature was then increased to 37°C to induce gelation, and a small amplitude oscillatory strain of 0.5% was imposed to track the gelation kinetics. After complete gelation, a creep test (1 Pa for 20 s) was performed to verify that there was no slip between the ECM hydrogels and rheometer plates.

Turbidometric gelation kinetics

The gelation kinetics of coECM hydrogels was evaluated turbidometrically.^{24,28} Briefly, neutralized pregel solutions of coECM at 4 and 8 mg/mL concentrations were prepared on ice. For each ECM concentration, 100 μL/well was added to a 96-well plate and placed into a plate reader (Spectramax M2, Molecular Devices, Sunnydale, CA) prewarmed to 37°C. Absorbance at 405 nm was read every 2 min for 60 min, and the readings were scaled from 0% (initial absorbance) to 100% (maximum absorbance). The time to half gelation

($t_{1/2}$) was defined as the time at 50% absorbance. Gelation rate was defined as the slope of the linear region of the gelation curve. The lag time (t_{lag}) was defined as the intercept of the linear region of the gelation curve with 0% absorbance.

In vitro cytocompatibility

In vitro cytocompatibility was determined using a LIVE/DEAD Viability/Cytotoxicity Kit (Invitrogen) following the manufacturer's directions. Briefly, 1 cm² multilaminates of coECM, XL-coECM, or scraped native colon were sterilized with ethylene oxide; 8 mg/mL coECM hydrogels were prepared as described earlier. Intestinal epithelial cells (IEC6; ATCC) were cultured and maintained in complete growth media consisting of 5% fetal bovine serum (FBS) (Gibco), 0.1 U/mL bovine insulin, 100 μg/mL penicillin, 100 U/mL streptomycin. IECs were seeded at 1×10^6 cells/scaffold for 48 h. Cell viability was compared with growth on tissue culture plastic (TCP). Cells were stained with 4 mM green fluorescent calcein-AM (cAM) and 2 mM red fluorescent ethidium homodimer (EthD)-1 to detect viable and dead cells, respectively. Images were taken with a Zeiss Axiovert microscope capturing three random fields across the scaffold. Quantification of percentage of live and dead cells was completed using a custom CellProfiler pipeline. Cell-seeded scaffolds were then fixed in 2% paraformaldehyde, embedded in paraffin, and sectioned for hematoxylin and eosin (H&E) staining.

In vitro macrophage response

Primary murine bone marrow-derived macrophages were isolated as described previously.²⁹ Briefly, bone marrow was isolated from the femur and tibia of C57bl/6 mice and cultured for 7 days in 100 ng/mL macrophage colony-stimulating factor (MCSF) to derive naïve (MΦ) macrophages. Macrophages were then activated with 20 ng/mL interferon (IFN)γ and 100 ng/mL lipopolysaccharide (LPS) to derive M1 macrophages, 20 ng/mL interleukin (IL)-4 to derive M2 macrophages, or 200 μg/mL of solubilized coECM for 18 h. Macrophages were then fixed with 2% paraformaldehyde for immunolabeling or lysed for western blot analysis. Cells were incubated in blocking buffer consisting of 0.1% Triton-X 100, 0.1% Tween-20, 2% bovine serum albumin (BSA), and 4% goat serum for 1 h at room temperature. Following blocking, cells were incubated in the following primary antibodies diluted in blocking buffer for 16 h at 4°C: (1) anti-F4/80 (Abcam) at 1:200, (2) anti-iNOS (Abcam) at 1:100,³⁰ or (3) anti-RELMα (Fizz1, Peprotech) at 1:200. Cells were washed with PBS and incubated in secondary antibodies diluted in blocking solution for 1 h at room temperature: (1) Alexa Fluor 488 goat anti-rat at 1:200 and (2) AlexaFluor 488 donkey anti-rabbit at 1:200. Cells were then washed with PBS and counterstained with DAPI nuclear stain. The assay was completed on four separate days ($n = 4$), and cells were imaged using a Zeiss Axiovert microscope with exposure times standardized using classically polarized (IFNy/LPS or IL-4) internal controls.

Percentage of F4/80, iNOS, and Fizz1 positive cells were quantified using CellProfiler.

Western blotting was performed to analyze an additional marker of M2 macrophages. Cells were lysed and lysates were boiled at 95°C for 5 min and loaded at 100 µg/well in a 4–20% gradient polyacrylamide SDS page gel. Separated proteins were transferred to PVDF membranes using a wet-transfer set up and incubated for 16 h in 3% milk, TBS-T to prevent nonspecific antibody binding. Membranes were incubated in the following primary antibodies for 18 h in 3% milk at 4°C: (1) polyclonal anti-rabbit mannose receptor (Abcam, Cambridge, MA) at 1:714 dilution for an M2 marker or (2) monoclonal anti-mouse β-actin (Santa Cruz, Dallas, TX) at a dilution of 1:1000 as a loading control. Three blots completed on separate days ($n = 3$) and were visualized using a LICOR Odyssey fluorescent imaging scanner. Densitometry of protein expression was standardized to the loading control.

***In vivo* cytocompatibility**

Thirty-two female Sprague-Dawley rats, weighing approximately 300 g, were randomly assigned to four groups based on test article (submucosa, coECM scaffold, XL-coECM scaffold, or coECM hydrogel) to characterize the host response to the implanted material. The test article was implanted in a rodent partial thickness abdominal wall defect model and animals were sacrificed at 14 d and 35 d postsurgery ($n = 4$ per time point per experimental group).

Abdominal wall defect model. The partial-thickness abdominal wall defect model for evaluation of the host response to biomaterials is well established.^{16,31} Surgical plane of anesthesia was achieved via inhalation of 2% isoflurane in oxygen. The surgical site was prepared by shaving the lateral abdominal region on both sides of each animal, followed by scrubbing and draping. Animals were placed in a lateral decubitus position and incisions made along the midaxillary line. The skin and subcutaneous tissues medial to the incision were separated from the underlying muscle tissues. A 1.5-cm × 1.5-cm section of the external and internal oblique layers of the ventral lateral abdominal wall were excised, while the underlying transversalis fascia and peritoneum were left intact. The muscle defect was subsequently repaired with a size-matched piece of the chosen test article or a hydrogel. The test articles were secured in place with 4–0 Prolene at each of the four corners securing the device to the surrounding and underlying musculature allowing for mechanical loading of the test article during the normal abdominal wall activity of daily living and facilitating identification at the time of explantation. Incisions were closed with 4–0 Vicryl sutures. Animals were recovered from anesthesia, returned to the housing unit, and received 0.02 mg Buprenex (buprenorphine hydrochloride) by subcutaneous injection the day of surgery and for two additional days twice daily. Baytril (20 mg) was administered orally the day of surgery and for two additional days. The dietary habits, general health status, and the surgical site were monitored daily and recorded. The implant site containing test articles

and surrounding adjacent tissue were isolated and placed in 10% neutral buffered formalin (NBF). Samples were then embedded in paraffin and cut into 6-µm sections for histologic studies.

Histomorphologic scoring. Tissue sections were stained with H&E for qualitative and semiquantitative histomorphologic analysis of remodeling outcomes. Two blinded investigators scored sections according to an established semiquantitative scoring method as shown in Table I. Scoring criteria were used to group devices according to the following categories: chronic inflammation and foreign body reaction (quantitative score < 5), early inflammatory cell infiltration with decreased cellularity and little evidence of constructive downstream remodeling (5 ≤ quantitative score ≤ 10), and early infiltration by inflammatory cells and signs of constructive remodeling at later time points (quantitative score > 10).

Host response: macrophage immunolabeling

The macrophage response to implanted test articles at 14 d postsurgery was characterized by immunolabeling. Heat-mediated antigen retrieval was performed in heated citrate buffer for 20 min (10 mM citrate, pH 6.0 at 95–100°C) on deparaffinized tissue sections. Tissue sections were allowed to cool and were incubated in blocking solution consisting of 2% goat serum, 1% BSA (Sigma), 0.1% Triton X-100 (Sigma), and 0.1% Tween-20 (Sigma) in PBS to prevent nonspecific antibody binding. After blocking, tissue sections were incubated with primary antibodies diluted 1:150 in blocking solution overnight at 4°C. CD68 (mouse anti-rat CD68 clone ED1; AbD Serotec) was used as a pan-macrophage marker, CD86 (rabbit anti-human CD86, clone EP 1158Y; Abcam) was used as an M1 macrophage marker, and CD206 (goat anti-human CD206 polyclonal; Santa Cruz) was used as an M2 marker. Following primary incubation, sections were washed in PBS and incubated in the following fluorescently conjugated secondary antibodies for 1 h at room temperature diluted in blocking solution: AlexaFluor donkey anti-mouse 594 at 1:200 (Invitrogen), PerCP-Cy5.5 donkey anti-rabbit at 1:300 (Santa Cruz), and AlexaFluor donkey anti-goat 488 at 1:200 (Invitrogen). Tissue sections were washed, counterstained with DAPI, and coverslipped. Multispectral images were acquired with appropriate filter sets using a Nuance microscope and spectrally unmixed to remove tissue autofluorescence. Four images were taken along the defect and underlying transversalis interface at 200× magnification. Total cells expressing CD68 and either CD86 or CD206 were quantified using CellProfiler image analysis software. Macrophages were defined as CD68 positive colocalized with nuclei. M1 and M2 cells were defined as macrophages (CD68⁺) coexpressing CD86 or CD206, respectively. Cells expressing both CD86 and CD206 were subtracted from the M1 and M2 totals, and an M2:M1 ratio was calculated for each image.

TABLE I. Histomorphologic scoring criteria

Cellular Infiltration	3 >200 cells	2 100–200 cells	1 1–100 cells	0 0 cells
Day 14 scoring criteria (per 20× field of view)				
Tissue organization/ scaffold remaining	Highly organized tissue/no scaffold remaining	Moderately organized tissue/some scaffold remaining	Unorganized tissue/most scaffold remaining	Unorganized tissue/scaffold intact
Fibrotic encapsulation	No encapsulation	Minimal encapsulation	Moderate encapsulation	Dense encapsulation >5 cells
Foreign body giant cells	0 cells	1 cell	2–5 cells	
Number of blood vessels	>10 vessels	6–10 vessels	2–5 vessels	0–1 vessels
Day 35 scoring criteria (per 20× field of view)				
Tissue organization/ scaffold remaining	Highly organized tissue/no scaffold present	Moderately organized tissue/little to no scaffold present	Unorganized tissue/moderate scaffold present	Scaffold intact
Fibrotic encapsulation	No encapsulation	Minimal encapsulation	Moderate encapsulation	Dense encapsulation >5 cells
Foreign body giant cells	0 cells	1 cells	2–5 cells	
Site appropriate tissue deposition	Organized muscle tissue throughout scaffold implant site	Muscle cells present throughout scaffold implant site	Muscle cells limited to scaffold periphery	No muscle ingrowth

Statistical analysis

A two-tailed equal variance Student's *t* test was used to determine whether the DNA, phospholipid, GAGs, HA, collagen, growth factor, and mechanics of the coECM were different than that of native colon ($p < 0.05$). A *t* test was also used to determine differences in turbidometric and rheologic properties of 4 mg/mL versus 8 mg/mL coECM hydrogels. A one-way analysis of variance (ANOVA) with *post hoc* Tukey test was used to determine differences in the percentage of viable cells in culture, percentage of cells expressing macrophage phenotype markers, *in vivo* histologic scores, and *in vivo* macrophage phenotype ratio. All data are reported as mean ± standard error.

RESULTS

Decellularization efficacy

A protocol for effective decellularization of colonic submucosa was identified with the use of enzyme and detergent washes. Although previously described decellularization protocols for GI tissue (e.g., esophageal and small intestine) do not require delipidization,^{10,23} the porcine colonic submucosa had high lipid content [Figure 1(A)] and, thereby, required delipidization for effective decellularization. The degree of decellularization following the described method was assessed using previously established guidelines for decellularization.³² No intact nuclei were visible by H&E or DAPI staining following decellularization [Figure 1(A)]. The concentration of remnant DNA in coECM (43 ± 5.3 ng/mg) was markedly less ($p < 0.001$) than those in native colonic tissue (7435 ± 420 ng/mg) and native submucosa ($998 \pm$

31 ng/mg) [Figure 1(B)]. Residual DNA was present in fragments <200 bp in length [Figure 1(C)]. In addition to DNA content, phospholipid concentration in the coECM was used as an indicator of decellularization efficacy. The concentration of phospholipids, a fundamental component of cell membranes, in the coECM was 876 ± 105 nmol/g and was much lower ($p < 0.001$) than the native colon [Figure 1(D)].

Biochemical and structural properties of coECM

The preservation and spatial distribution of ECM proteins, including basement membrane-associated laminin and, a non-basement membrane protein, fibronectin, were examined. Immunolabeling expectedly showed that laminin was present along the basement membrane of the native colon but this layer was mechanically removed during decellularization, and, thus, laminin was largely absent in the coECM. Similarly, positive staining for fibronectin was present and distributed throughout the native colonic tissue but only diffuse staining for fibronectin was observed in the coECM [Figure 2(A)]. The surface ultrastructure of the coECM scaffold was observed with SEM. SEM images of the luminal and abluminal surface of coECM showed a smooth surface on the luminal surface of the coECM. The abluminal surface, however, had a more textured and fibrous appearance [Figure 2(B)].

Biochemical characterization of coECM showed that important ECM constituents are present in the decellularized colonic mucosa. GAGs, both sulfated and nonsulfated, were retained in coECM. A large percentage of sGAGs were preserved in the coECM although the concentration was less than ($p = 0.012$) the native tissue [Figure 3(A)]. HA, a

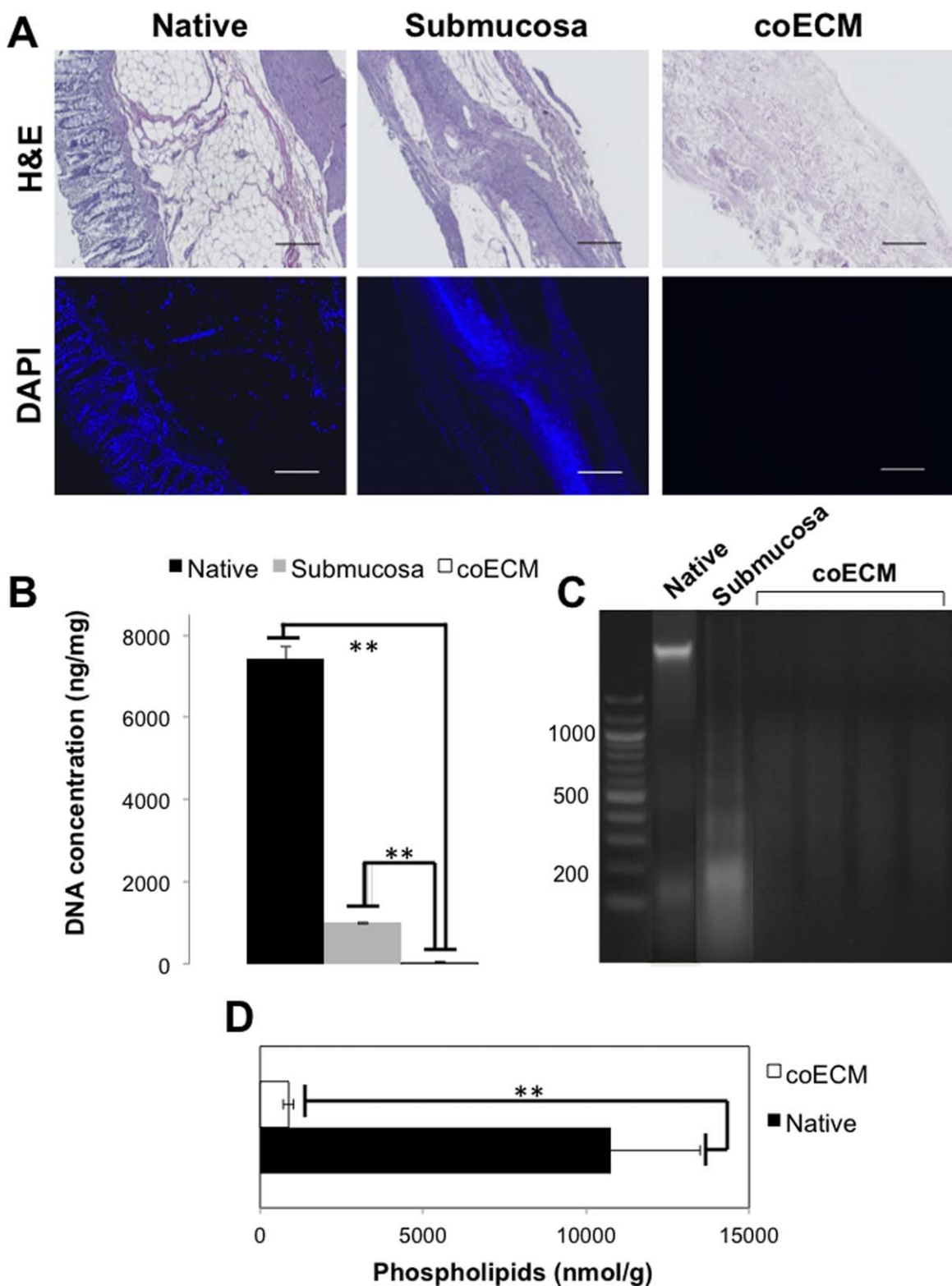


FIGURE 1. Decellularization efficacy. (A) The presence of nuclei in the decellularized tissue was assessed by hematoxylin and eosin (H&E) staining and 4',6-diamidino-2-phenylindole (DAPI) staining. (B) DNA concentration was quantified using PicoGreen® assay. (C) The fragment length of residual DNA was visualized by gel electrophoresis. (D) Residual cell membrane components were quantified using EnzyChrom™ phospholipid assay. Scale bar = 200 μ m. ** p < 0.01.

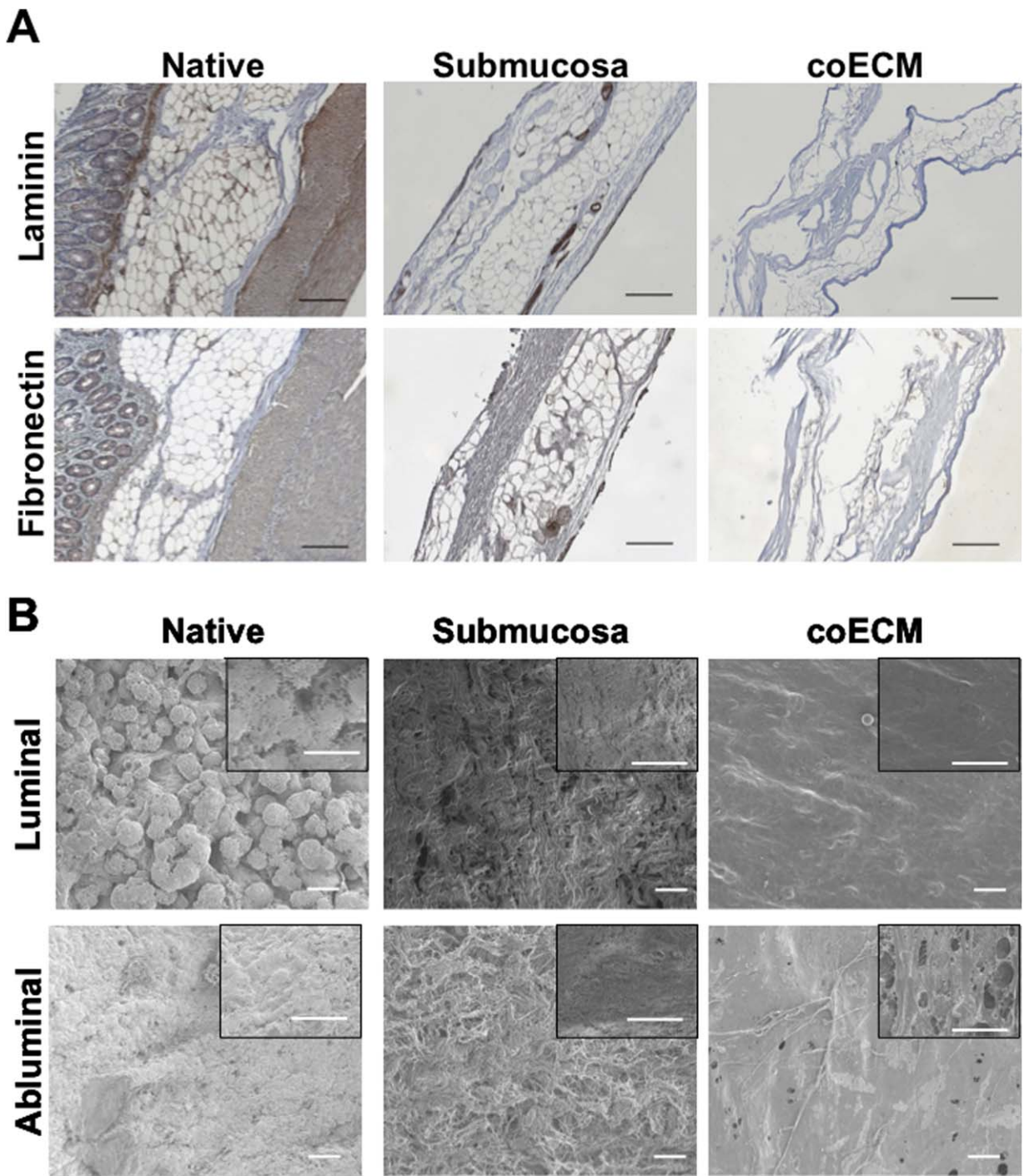


FIGURE 2. Composition and ultrastructure. (A) The presence and distribution of laminin and fibronectin was assessed by immunohistochemical staining. (B) The ultrastructure of the luminal and abluminal surfaces of the scaffold was visualized at low and high (inset) magnification. Scale bar in 2A = 200 μ m. Scale bar in 2B = 50 μ m.

nonsulfated GAG, was present in the coECM while the concentration was also lower ($p = 0.001$) than native tissue [Figure 3(B)]. The amount of fibrillar collagen in the coECM was expectedly greater ($p = 0.039$) than native tissue as collagen represents a large proportion of the ECM [Figure 3(C)]. Lastly, although present in reduced levels compared

with native tissue, both bFGF [Figure 3(D), $p < 0.001$] and VEGF [Figure 3(E), $p < 0.001$] were retained in the coECM.

Mechanical properties of coECM scaffold

The equibiaxial stress response of the native colon showed anisotropic behavior with a maximum strain of 4.9% and

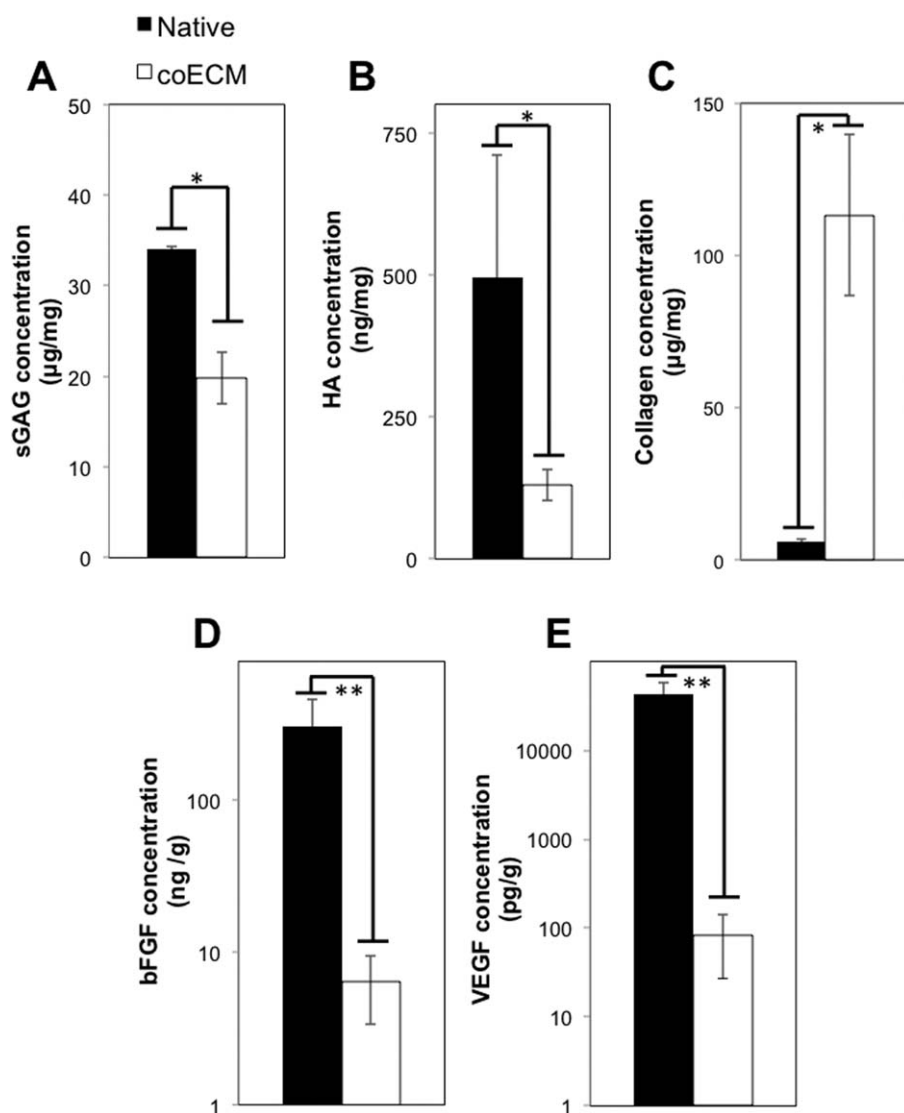


FIGURE 3. Biochemical composition. The retention of biochemical constituents in coECM was compared with native colonic tissue. (A) The concentration of sulfated glycosaminoglycans (sGAGs) was measured using Blyscan™ assay. (B) Nonsulfated GAG hyaluronic acid (HA) content was measured using an ELISA. (C) Fibrillar collagen was quantified using Sircol™ assay. The presence of two growth factors, bFGF (D) and VEGF (E), was detected using ELISA kits. * $p < 0.05$, ** $p < 0.01$.

2.4% in the longitudinal and circumferential direction, respectively [Figure 4(A,B)]. The coECM showed similar anisotropy but had a lower compliance along both the longitudinal (1.8%, $p = 0.042$) and circumferential (0.5%, $p = 0.023$) axes [Figure 4(A,B)]. The multilaminate coECM scaffold, however, had marked increase ($p < 0.001$) in suture retention strength compared with the native colon [Figure 4(C)].

Rheologic and turbidometric properties of coECM hydrogel

The turbidometric and rheological properties of the coECM hydrogel were concentration dependent. Macroscopically, the higher ECM concentration (8 mg/mL) hydrogels had a rigid structure with defined edges and could be handled and manipulated with forceps, while the 4-mg/mL hydrogels were softer with rounded edges and not easily handled

[Figure 5(A)]. Compared with the 4-mg/mL hydrogel, the more-concentrated 8-mg/mL hydrogel had a shorter lag time (17 ± 0.3 vs. 22 ± 0.8 min; $p < 0.001$) prior to gelation [Figure 5(B)] and gelled more rapidly [Figure 5(C,D)]. Results of rheological testing showed that the 8-mg/mL pre-gel was more ($p = 0.027$) viscous [Figure 5(E)] and the hydrogel that formed was much stiffer ($p = 0.001$) than the 4-mg/mL hydrogel [Figure 5(F)].

In vitro cell response to coECM

Intestinal epithelial cells retained nearly 100% viability when seeded on coECM, XL-coECM, coECM gel, and submucosa [Figure 6(A)]. There was no difference between these treatments and when compared with tissue culture plastic after 24 h in culture [Figure 6(B)].

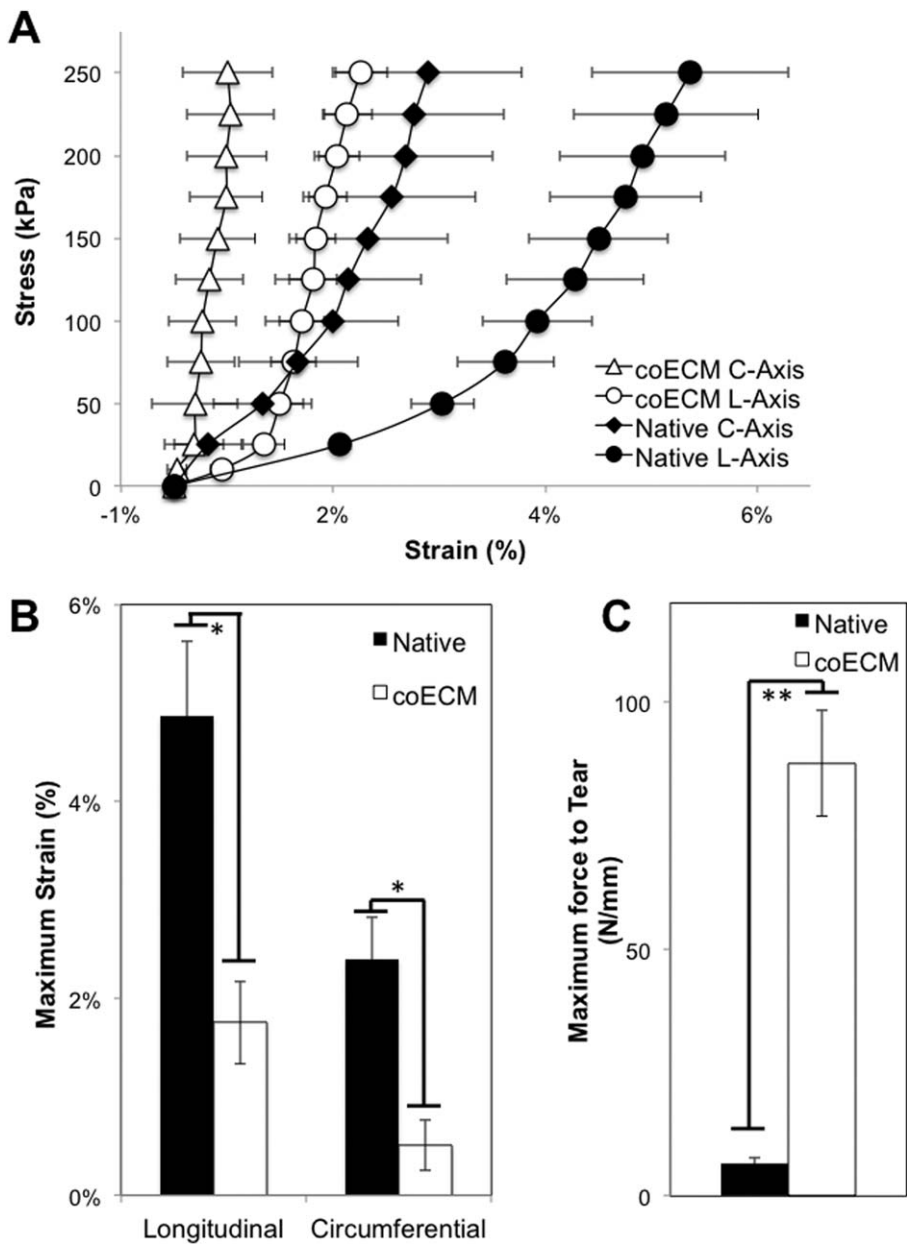


FIGURE 4. Scaffold mechanical properties. (A) The response of the scaffold to equibiaxial stress was assessed using planar biaxial testing. (B) Maximum strain of the scaffold at a stress of 250 kPa was quantified in the longitudinal and circumferential direction. (C) The suture retention strength of multilaminate scaffolds was compared prior to *in vivo* implantation. * $p < 0.05$, ** $p < 0.01$.

Primary murine bone marrow-derived macrophages were activated to the M1 (IFN γ /LPS) and M2 (IL-4) phenotypes for 18 h or treated with 200 μ g/mL of solubilized coECM. All experimental groups showed uniform F4/80 staining with $93.4 \pm 0.5\%$ of cells expressing the pan-macrophage marker. The controls showed an expected increase ($p < 0.001$) in iNOS when macrophages were treated with IFN γ /LPS and an increase ($p < 0.001$) inFizz1 when treated with IL-4. The coECM treatment was found to promote M2-like macrophage activation, similar to IL-4-treated macrophages as shown by Fizz1 expression accompanied by little iNOS expression [Figure 6(C)]. Results quantified using CellProfiler show a large Fizz1+ cell population and small iNOS+ cell population when treated with coECM, sug-

gesting that coECM directly promotes a constructive, M2-like macrophage phenotype [Figure 6(D)]. The presence of CD206, a cell surface receptor that is indicative of M2 macrophage phenotype, was assessed using western blot analysis and normalized to a β -actin loading control. Similar to above with Fizz1 expression, the ratio of CD206: β -actin was on average greatest in macrophages following IL-4 (1.8 ± 0.4) and coECM treatment (1.2 ± 0.2) compared with IFN γ /LPS treatment (0.6 ± 0.2) or the pepsin control, although not significant.

In vivo host response

The *in vivo* host response to coECM was examined in a rat abdominal wall defect model at both 14 and 35 d following

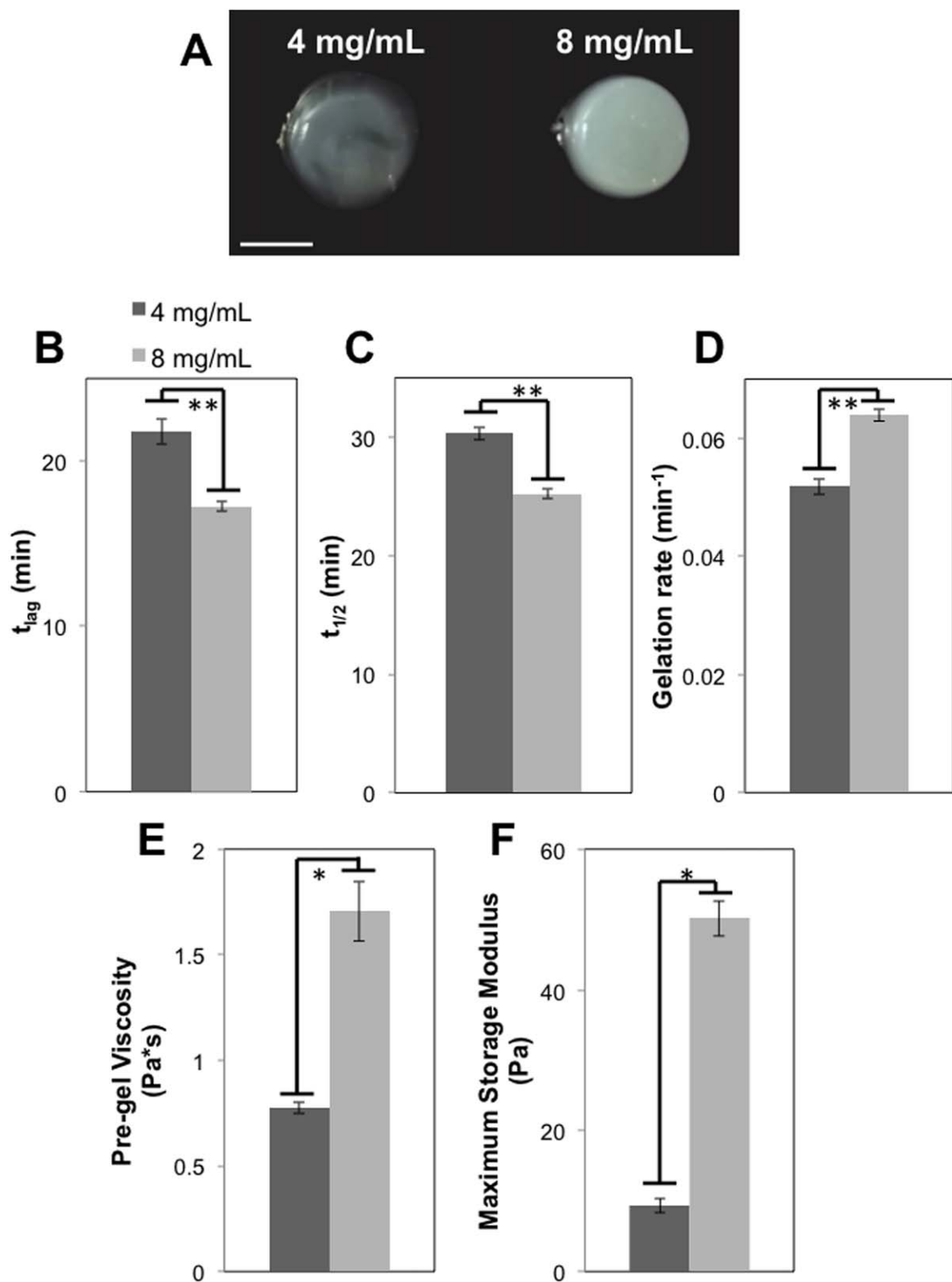


FIGURE 5. Hydrogel turbidometric and rheological properties. (A) Two concentrations of coECM hydrogel, 4 and 8 mg/mL, were formed in a ring mold and compared macroscopically. Turbidometric analysis was used to measure the t_{lag} (B), $t_{1/2}$ (C), and rate of gelation (D) of the hydrogel at two different concentrations. Parallel plate rheology was used to measure the viscosity of the pregel (E) and maximum storage modulus of the hydrogel (F). Scale bar = 1 cm, * $p < 0.05$, ** $p < 0.01$.

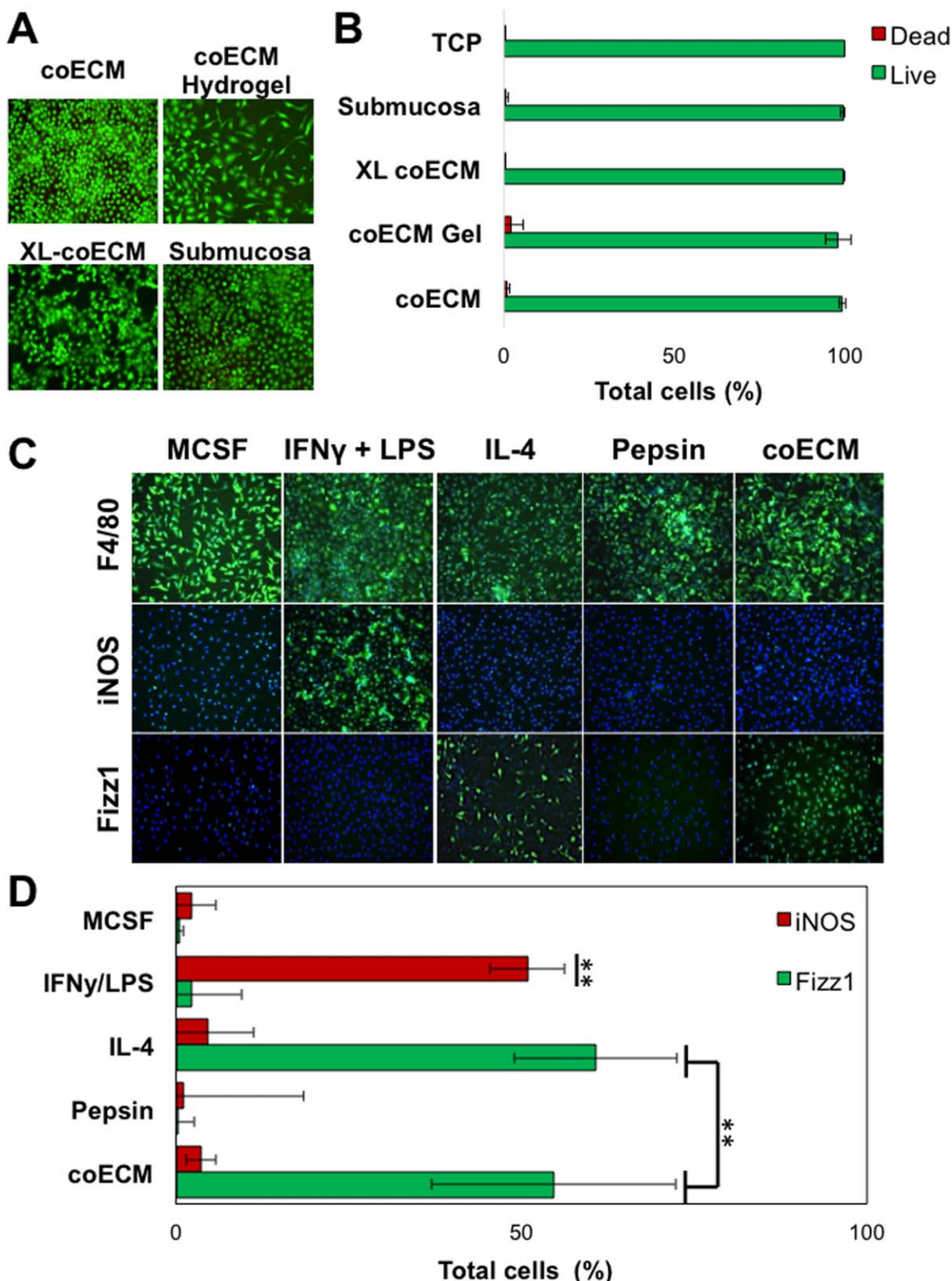


FIGURE 6. *In vitro* cell response. (A) Intestinal epithelial cells cultured on coECM scaffold, coECM hydrogel, XL-coECM, and native submucosa were stained with LIVE/DEAD® cell viability dye and (B) the percentage of live and dead cells were quantified. (C) Bone marrow-derived macrophages were cultured in the presence of enzymatically digested coECM and immunolabeled for F4/80 (pan macrophage), iNOS (M1), and Fizz1 (M2). Controls included MCSF (baseline), IFN γ +LPS (M1), IL-4 (M2), and pepsin (digestion buffer). (D) The percentage of cells expressing the markers indicative of M1 and M2 phenotypes was quantified and compared. ** $p < 0.01$.

implantation. In addition to coECM and coECM hydrogel, two additional groups were used as negative controls. Native colonic submucosa was used as a control to validate the necessity for effective decellularization.¹⁰ Crosslinked coECM was used to validate the need for scaffold degradation.⁶ By 14 d, coECM sheet and gel implants showed histologic evidence of a robust cell infiltrate (cell infiltrate score of 3 and 2.5, respectively) and partial scaffold degradation (degradation score of 2 and 2.6, respectively) shown by H&E staining [Figure 7(A)]. The average cumulative histologic score for coECM sheet was 12.9 and coECM gel was 12.1 [Figure 7(B)]. In contrast, crosslinked coECM and native colonic submucosa implants were characterized by very little cellular infiltration (each with a cell infiltrate score of 2) and vessel formation (vasularity score of 2 and 1.5, respectively) and minimal scaffold degradation [Figure 7(A)]. Disorganized connective tissue was present along the interface of XL-coECM and submucosa with the native underlying muscle. The average cumulative histologic scores for XL-coECM and native submucosa was 9.4 and 8.8, respectively [Figure 7(B)], which were both significantly less ($p < 0.05$) than the coECM and coECM hydrogel. By 35 d, coECM sheets and gels were completely degraded (tissue organization scores of 2 and 2.25, respectively) while XL-coECM and native colonic submucosa remained almost completely intact and had tissue organization scores of 1.6 and 1.5, respectively [Figure 7(A)]. The cumulative histologic scores for both coECM and coECM hydrogel were greater ($p < 0.05$) than both XL-coECM and native submucosa [Figure 7(B)].

Macrophage immunolabeling at 7 d postsurgery [Figure 7(C)] showed a predominant CD68⁺CD206⁺ M2 macrophage population in coECM sheet and gel-treated groups when compared with a predominant CD68⁺CD86⁺ proinflammatory M1 macrophage phenotype following XL-coECM or colonic submucosa implantation as shown in Figure 7(C). The ratio of the M2:M1 macrophages in the coECM scaffold was 1.46 ± 0.3 , which was greater ($p < 0.01$) than the XL-coECM and native submucosa [Figure 7(D)]. The M2:M1 ratio in the coECM gel was on average also greater than the XL-coECM and native submucosa, although not significant ($p = 0.055$)

DISCUSSION

Functional replacement of injured or missing GI tissue requires a diverse tool set to promote the growth and differentiation of specialized cell types and tissue layers that vary from esophagus to small intestine to colon. This study represents a thorough characterization of an ECM bioscaffold derived from porcine colon (coECM). The coECM scaffold was shown to be decellularized—meeting previously established stringent criteria.³² The decellularization protocol effectively removed native DNA while preserving essential structural and biochemical ECM components including sGAGs, HA, collagen, bFGF, and VEGF. The coECM scaffold was shown to retain similar mechanical properties and anisotropy as native colon. *In vitro* and *in vivo* coECM is cyto-

compatible and promotes a constructive, M2-like macrophage phenotype when compared with its ineffectively decellularized or crosslinked counterparts. Such properties make coECM promising for use as an “off-the-shelf” GI repair biomaterial.

Regions of the GI tract, specifically the SIS and esophageal mucosa, have been successfully decellularized previously.^{23,33} Just as the native GI tract is a highly complex and variable organ, the composition and properties of each of these bioscaffolds are also variable. Such properties are largely dependent on the method of decellularization utilized and the source tissue from which they are derived. SIS-ECM is prepared primarily by mechanical delamination and exposure to peracetic acid. Esophageal ECM (eECM), on the other hand, is exposed to a series of enzymatic and chemical detergent treatments after mechanical delamination methods, similar to coECM preparation²³ though an additional delipidization step is necessary for coECM decellularization. Each of these protocols results in scaffolds with unique properties and compositions. For example, when compared with eECM, coECM has a lower maximum strain along the longitudinal axis.²³ Differences in these values could be important determinants of *in vivo* remodeling outcomes. Previous studies have shown that tensile strength increases from proximal to distal intestine,³⁴ likely stemming from the need of distal colon to accommodate changes in higher stress as fecal pellets become more solid. Distinguishing the mechanics of different regions of the gut and a thorough comparison and understanding of the similarities and differences between ECMs derived from different source tissues could have important implications for application-specific selection of bioscaffolds, particularly in GI repair applications, which are also inherently diverse and complex and require individualized mechanics for peristalsis, digestion, absorption, and gastric motility.

While heterologous ECM bioscaffolds have been used with success in multiple anatomic locations for constructive tissue remodeling, a subset of studies have indicated that it may be advantageous to utilize site-specific ECM.^{12,13,35–37} Each tissue has a distinct composition of ECM in which the appropriate signaling molecules and structural components are present to allow for cell growth and differentiation and synergized tissue function. It is reasonable to assume, therefore, that decellularization of site-specific tissue would provide the optimal inductive template for tissue engineering in its respective anatomic location. Whether or not site-specific ECM use is relevant in all therapeutic applications, however, is not fully understood. Results of this show coECM facilitated constructive tissue remodeling in a heterologous location. Design of a tissue-engineered intestine should take into consideration gut function such as contractility. Biomaterials for gut replacement should allow for regeneration of functional muscle and directional self-organization of functionally distinct layers that perform a variety of functions including nutrient absorption, mucus secretion, and motility. Future studies are warranted to determine the efficacy of coECM as a bioscaffold in gastrointestinal, or specifically colon, disease/injury models.

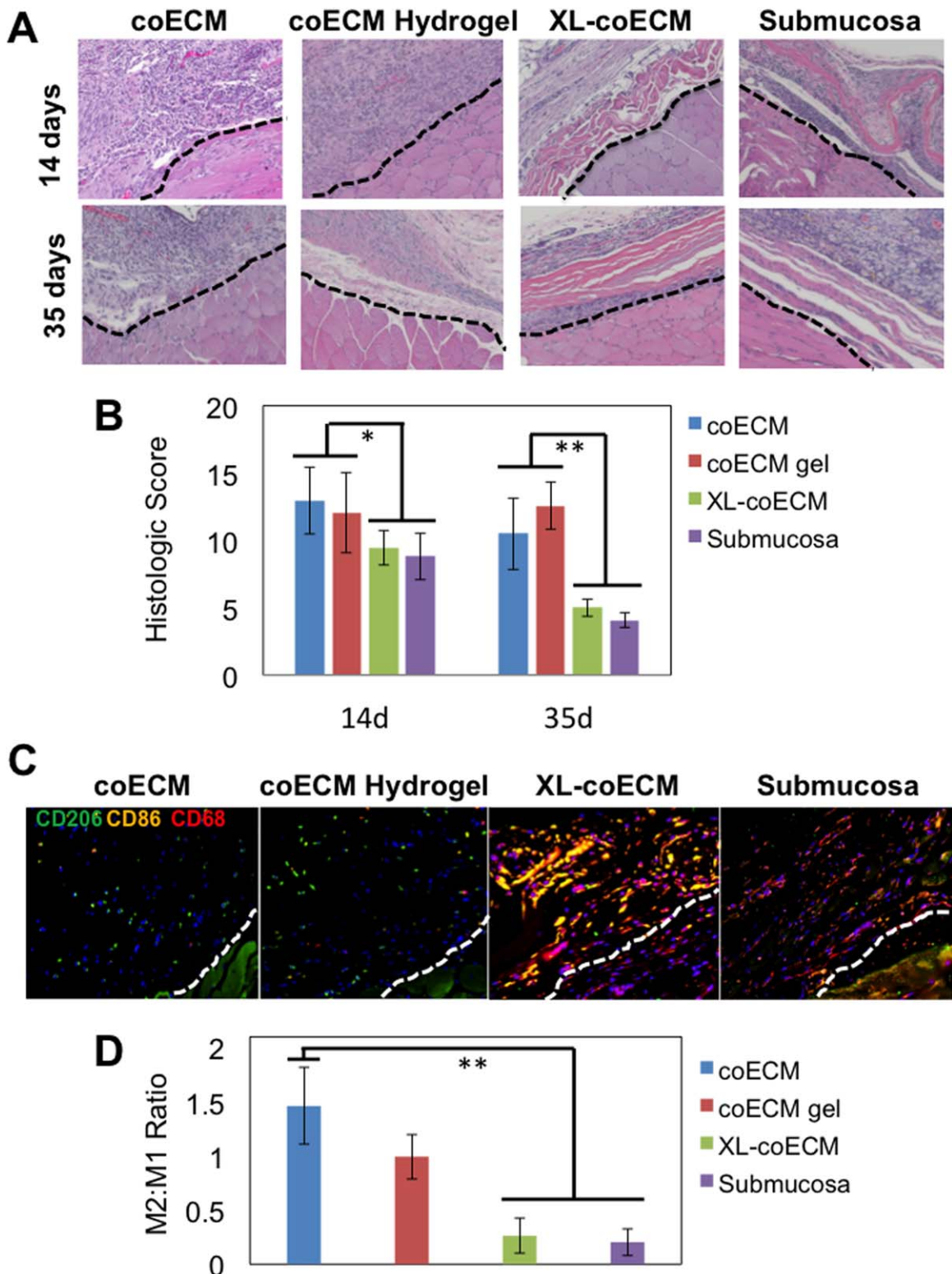


FIGURE 7. Host response. The host response to coECM scaffold and hydrogel was compared *in vivo* to XL-coECM and native submucosa in a rat abdominal defect model. (A) Representative H&E images show the histologic response at 14 and 35 days. (B) The combined histologic score at each time point was quantified and compared across groups. (C) The macrophage response at 14 days postsurgery was analyzed by immunofluorescent staining for M2 indicator CD206 (green), M1 indicator CD86 (orange), and pan-macrophage CD68 (red). (D) The ratio of M2 ($CD68^{+}/CD206^{+}$) to M1 ($CD68^{+}/CD86^{+}$) was quantified and compared across groups. Dashed lines indicate interface between scaffold and underlying muscle. * $p < 0.05$, ** $p < 0.01$.

Although the mechanism(s) of action of ECM-mediated tissue remodeling are only partially understood, the activation/polarization of infiltrating macrophages at the remodeling site from a proinflammatory, cytotoxic M1 phenotype to an immunoregulatory, constructive M2 macrophage phenotype has been shown to be a predictor of favorable downstream remodeling outcomes.³⁸ This study shows that coECM promotes a predominant M2 ($CD68^+CD206^+$) macrophage phenotype when compared with native colonic submucosa and XL-coECM following implantation. The immunomodulatory properties of coECM may prove beneficial in cases of inflammatory bowel disease treatment in which it is postulated that the host lamina propria macrophages fail to polarize toward a more-tolerant M2-like phenotype.^{39,40} This study shows that coECM can also be prepared in a hydrogel form with unique and concentration-dependent viscoelastic properties, providing flexibility for *in vivo* applications such as injectable or enema administration.

Biologic scaffolds are preferred over synthetic scaffolds for many tissue repair applications because of their degradability *in vivo*. It is now well accepted that crosslinking biologic scaffolds results in slower degradation and often encapsulation and fibrosis. Such inhibition of scaffold degradation prevents the release or exposure of matrixryptic peptides and is consistently associated with less than desirable outcomes.^{31,41} H&E staining of abdominal wall explants shows that coECM sheet and hydrogel formulations are characterized by a robust cellular infiltrate at 14 d and are largely degraded by 35 d, unlike the native (nondecellularized) submucosa and XL-coECM, which were characterized by mostly disorganized connective tissue and some encapsulation as reflected by a lower histomorphologic score. This score differential is likely due to the incomplete decellularization of the submucosa graft and the inability of XL-coECM to degrade. Ineffective decellularization has been shown to be a crucial factor in provoking a foreign body reaction from the host following bioscaffold implantation.^{10,42} Degradation products of coECM have been shown to not only promote a predominant F480⁺/Fizz1⁺ macrophage population *in vitro*, but previous work has also shown that degradation products of ECM are chemotactic and mitogenic for progenitor cells both *in vitro* and *in vivo*.^{9,29,43} These results emphasize the importance for effective decellularization and scaffold degradation.

This study has limitations. While coECM was shown to be conducive to intestinal epithelial cell survival *in vitro*, the tissue-specific effects of coECM on colonic progenitor cells and in a colonic repair animal model were not evaluated. In addition, while retention of growth factors bFGF and VEGF protein were measured, their bioactivity was not measured. The role of these growth factors in constructive remodeling is not understood. Previous work shows that vascularization has been, to this point, a limiting step in tissue-engineered construct survival.³ Future studies should determine whether coECM-retained VEGF remains active to promote an angiogenic response. While a high M2:M1 macrophage ratio has been shown to be a predictor of downstream remodeling outcomes in ECM-mediated tissue repair, macro-

phage phenotype polarizes along a spectrum. This study utilizes CD206 and CD86 for M2 and M1 macrophage markers, respectively; however, a more thorough characterization of macrophage activation phenotype would result from analyzing additional markers.

CONCLUSION

A biologic scaffold was successfully prepared from porcine colon. The coECM scaffold was effectively decellularized and retained important ECM constituents. The decellularized tissue was prepared in hydrogel or lyophilized sheet forms to address diverse gastrointestinal repair applications. Both forms of ECM were conducive to intestinal epithelial cell growth and were shown to promote a constructive macrophage phenotype *in vitro*. Surgically implanted coECM scaffold and hydrogel also promote an immunomodulatory host response and site appropriate tissue deposition. Given the large unmet clinical need for repair of GI tissue, further work is warranted to examine the specific effects of coECM upon colonic stem/progenitor cells and *in vivo* remodeling in a GI disease model to assess site-specific effects of ECM bioscaffolds.

REFERENCES

1. Loftus EV, Jr. Clinical epidemiology of inflammatory bowel disease: Incidence, prevalence, and environmental influences. *Gastroenterology* 2004;126:1504–1517.
2. Byrne TA, Persinger RL, Young LS, Ziegler TR, Wilmore DW. A new treatment for patients with short-bowel syndrome. Growth hormone, glutamine, and a modified diet. *Ann Surg* 1995;222:243–254; discussion 54–55.
3. Bitar KN, Raghavan S. Intestinal tissue engineering: Current concepts and future vision of regenerative medicine in the gut. *Neurogastroenterol Motil* 2012;24:7–19.
4. Shin H, Jo S, Mikos AG. Biomimetic materials for tissue engineering. *Biomaterials* 2003;24:4353–4364.
5. Anderson JM, Rodriguez A, Chang DT. Foreign body reaction to biomaterials. *Semin Immunol* 2008;20:86–100.
6. Brown BN, Valentin JE, Stewart-Akers AM, McCabe GP, Badylak SF. Macrophage phenotype and remodeling outcomes in response to biologic scaffolds with and without a cellular component. *Biomaterials* 2009;30:1482–1491.
7. Sicari BM, Johnson SA, Siu BF, Crapo PM, Daly KA, Jiang H, Medberry CJ, Tottey S, Turner NJ, Badylak SF. The effect of source animal age upon the *in vivo* remodeling characteristics of an extracellular matrix scaffold. *Biomaterials*. 2012;33:5524–5533.
8. Valentin JE, Stewart-Akers AM, Gilbert TW, Badylak SF. Macrophage participation in the degradation and remodeling of extracellular matrix scaffolds. *Tissue Eng Part A* 2009;15:1687–94.
9. Reing JE, Zhang L, Myers-Irvin J, Cordero KE, Freytes DO, Heber-Katz E, Bedelbaeva K, McIntosh D, Dewilde A, Brauhut SJ, Badylak SF. Degradation products of extracellular matrix affect cell migration and proliferation. *Tissue Eng Part A* 2009;15:605–614.
10. Keane TJ, Londono R, Turner NJ, Badylak SF. Consequences of ineffective decellularization of biologic scaffolds on the host response. *Biomaterials* 2012;33:1771–1781.
11. Hodde JP, Record RD, Tullius RS, Badylak SF. Retention of endothelial cell adherence to porcine-derived extracellular matrix after disinfection and sterilization. *Tissue Eng* 2002;8:225–234.
12. Sellaro TL, Ranade A, Faulk DM, McCabe GP, Dorko K, Badylak SF, Strom SC. Maintenance of human hepatocyte function *in vitro* by liver-derived extracellular matrix gels. *Tissue Eng Part A* 2010;16:1075–1082.
13. Sellaro TL, Ravindra AK, Stoltz DB, Badylak SF. Maintenance of hepatic sinusoidal endothelial cell phenotype *in vitro* using

- organ-specific extracellular matrix scaffolds. *Tissue Eng* 2007;13:2301–10.
14. Medberry CJ, Crapo PM, Siu BF, Carruthers CA, Wolf MT, Nagarkar SP, Agrawal V, Jones KE, Kelly J, Johnson SA, Velankar SS, Watkins SC, Modo M, Badylak SF. Hydrogels derived from central nervous system extracellular matrix. *Biomaterials* 2013;34:1033–1040.
 15. French KM, Boopathy AV, DeQuach JA, Chingozha L, Lu H, Christman KL, Davis ME. A naturally derived cardiac extracellular matrix enhances cardiac progenitor cell behavior in vitro. *Acta Biomater* 2012;8:4357–4364.
 16. Badylak S, Kokini K, Tullius B, Simmons-Byrd A, Morff R. Morphologic study of small intestinal submucosa as a body wall repair device. *J Surg Res* 2002;103:190–202.
 17. Chen MK, Badylak SF. Small bowel tissue engineering using small intestinal submucosa as a scaffold. *J Surg Res* 2001;99:352–358.
 18. Cobb MA, Badylak SF, Janas W, Simmons-Byrd A, Boop FA. Porcine small intestinal submucosa as a dural substitute. *Surg Neurol* 1999;51:99–104.
 19. Badylak SF, Kropp B, McPherson T, Liang H, Snyder PW. Small intestinal submucosa: A rapidly resorbed bioscaffold for augmentation cystoplasty in a dog model. *Tissue Eng* 1998;4:379–387.
 20. Badylak SF, Record R, Lindberg K, Hodde J, Park K. Small intestinal submucosa: A substrate for in vitro cell growth. *J Biomater Sci Polym Ed* 1998;9:863–878.
 21. Prevel CD, Eppley BL, Summerlin DJ, Sidner R, Jackson JR, McCarty M, Badylak SF. Small intestinal submucosa: Utilization as a wound dressing in full-thickness rodent wounds. *Ann Plast Surg* 1995;35:381–388.
 22. Prevel CD, Eppley BL, Summerlin DJ, Jackson JR, McCarty M, Badylak SF. Small intestinal submucosa: Utilization for repair of rodent abdominal wall defects. *Ann Plast Surg* 1995;35:374–380.
 23. Keane TJ, Londono R, Carey RM, Carruthers CA, Reing JE, Dearth CL, D'Amore A, Medberry CJ, Badylak SF. Preparation and characterization of a biologic scaffold from esophageal mucosa. *Biomaterials* 2013;34:6729–6737.
 24. Freytes DO, Martin J, Velankar SS, Lee AS, Badylak SF. Preparation and rheological characterization of a gel form of the porcine urinary bladder matrix. *Biomaterials* 2008;29:1630–1637.
 25. Wolf MT, Carruthers CA, Dearth CL, Crapo PM, Huber A, Burnsed OA, Londono R, Johnson SA, Daly KA, Stahl EC, Freund JM, Medberry CJ, Carey LE, Nieponice A, Amoroso NJ, Badylak SF. Polypropylene surgical mesh coated with extracellular matrix mitigates the host foreign body response. *J Biomed Mater Res A* 2013;102:234–246.
 26. Billiar KL, Sacks MS. Biaxial mechanical properties of the natural and glutaraldehyde treated aortic valve cusp—Part I: Experimental results. *J Biomech Eng* 2000;122:23–30.
 27. Freytes DO, Tullius RS, Badylak SF. Effect of storage upon material properties of lyophilized porcine extracellular matrix derived from the urinary bladder. *J Biomed Mater Res B Appl Biomater* 2006;78:327–333.
 28. Wolf MT, Daly KA, Brennan-Pierce EP, Johnson SA, Carruthers CA, D'Amore A, Nagarkar SP, Velankar SS, Badylak SF. A hydrogel derived from decellularized dermal extracellular matrix. *Biomaterials*. 2012;33:7028–7038.
 29. Sicari BM, Dziki JL, Siu BF, Medberry CJ, Dearth CL, Badylak SF. The promotion of a constructive macrophage phenotype by solubilized extracellular matrix. *Biomaterials* 2014;35:8605–8612.
 30. Lee AC, Yu VM, Lowe JB III, Brenner MJ, Hunter DA, Mackinnon SE, Sakiyama-Elbert SE. Controlled release of nerve growth factor enhances sciatic nerve regeneration. *Exp Neurol* 2003;184:295–303.
 31. Valentin JE, Badylak JS, McCabe GP, Badylak SF. Extracellular matrix bioscaffolds for orthopaedic applications. A comparative histologic study. *J Bone Joint Surg Am* 2006;88:2673–2686.
 32. Crapo PM, Gilbert TW, Badylak SF. An overview of tissue and whole organ decellularization processes. *Biomaterials* 2011;32:3233–3243.
 33. Badylak S, Kokini K, Tullius B, Whitson B. Strength over time of a resorbable bioscaffold for body wall repair in a dog model. *J Surg Res* 2001;99:282–287.
 34. Watters DA, Smith AN, Eastwood MA, Anderson KC, Elton RA. Mechanical properties of the rat colon: the effect of age, sex and different conditions of storage. *Q J Exp Physiol* 1985;70:151–162.
 35. Cheng NC, Estes BT, Awad HA, Guilak F. Chondrogenic differentiation of adipose-derived adult stem cells by a porous scaffold derived from native articular cartilage extracellular matrix. *Tissue Eng Part A* 2009;15:231–241.
 36. Cortiella J, Niles J, Cantu A, Brettler A, Pham A, Vargas G, Winston S, Wang J, Walls S, Nichols JE. Influence of acellular natural lung matrix on murine embryonic stem cell differentiation and tissue formation. *Tissue Eng Part A* 2010;16:2565–2680.
 37. Zhang Y, He Y, Bharadwaj S, Hammam N, Carnagey K, Myers R, Atala A, Van Dyke M. Tissue-specific extracellular matrix coatings for the promotion of cell proliferation and maintenance of cell phenotype. *Biomaterials* 2009;30(23–24):4021–4028.
 38. Brown BN, Londono R, Tottey S, Zhang L, Kukla KA, Wolf MT, Daly KA, Reing JE, Badylak SF. Macrophage phenotype as a predictor of constructive remodeling following the implantation of biologically derived surgical mesh materials. *Acta Biomater* 2012;8:978–987.
 39. Wang W, Li X, Zheng D, Zhang D, Peng X, Zhang X, Ai F, Wang X, Ma J, Xiong W, Li G, Zhou Y, Shen S. Dynamic changes and functions of macrophages and M1/M2 subpopulations during ulcerative colitis-associated carcinogenesis in an AOM/DSS mouse model. *Mol Med Rep* 2015;11:2397–2406.
 40. Cosín-Roger J, Ortiz-Masiá D, Calatayud S, Hernández C, Alvarez A, Hinojosa J, Esplugues JV, Barrachina MD. M2 macrophages activate WNT signaling pathway in epithelial cells: relevance in ulcerative colitis. *PLoS One* 2013;8:e78128.
 41. Valentin JE, Turner NJ, Gilbert TW, Badylak SF. Functional skeletal muscle formation with a biologic scaffold. *Biomaterials* 2010;31:7475–7484.
 42. Keane TJ, Swinehart I, Badylak SF. Methods of tissue decellularization used for preparation of biologic scaffolds and in-vivo relevance. *Methods* 2015;84:25–34.
 43. Vorotnikova E, McIntosh D, Dewilde A, Zhang J, Reing JE, Zhang L, Cordero K, Bedelbaeva K, Gourevitch D, Heber-Katz E, Badylak SF, Brauhut SJ. Extracellular matrix-derived products modulate endothelial and progenitor cell migration and proliferation in vitro and stimulate regenerative healing in vivo. *Matrix Biol* 2010;29:690–700.